

NLO QCD corrections to $t\bar{t}b\bar{b}$ production at the LHC

Ansgar Denner, PSI

Loops and Legs, Wörlitz, April 25-30, 2010

in collaboration with A. Bredenstein, S. Dittmaier, S. Pozzorini

- Motivation
- Some details of the calculations
- Numerical results
- Conclusion

$2 \rightarrow 4$ processes of Les Houches 2005/2007 priority list

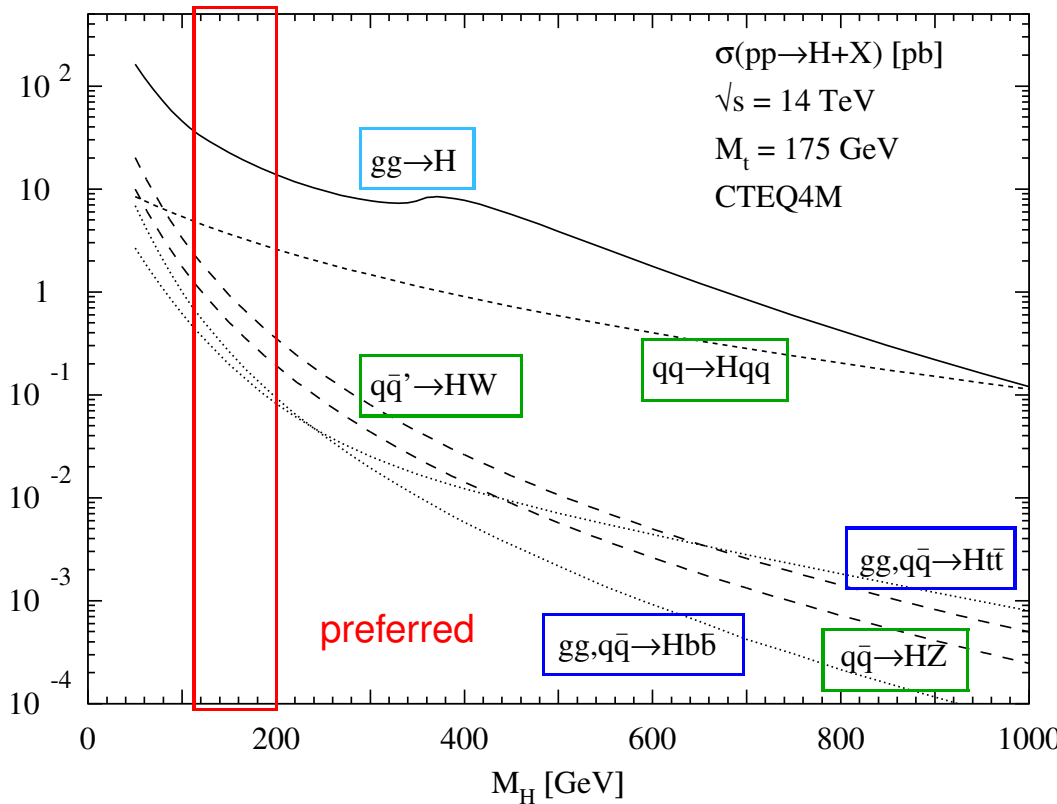
Big progress during last 2 years

reaction	existing calculations	method
$pp \rightarrow t\bar{t}bb$	Bredenstein, Denner, Dittmaier, Pozzorini '09 Bevilacqua, Czakon, Papadopoulos, Pittau, Worek '09	Feynman diagrams OPP reduction and HELAC
$pp \rightarrow t\bar{t}jj$	Bevilacqua, Czakon, Papadopoulos, Worek '10	OPP reduction and HELAC
$pp \rightarrow VVbb$	–	
$pp \rightarrow VVjj$	–	
$pp \rightarrow Wjjj$	Berger et al. '09 R.K.Ellis et al. '09 (leading colour)	generalized unitarity <i>D</i> -dimensional unitarity
$pp \rightarrow Zjjj$	Berger et al. '10	generalized unitarity
$pp \rightarrow b\bar{b}b\bar{b}$	Binoth et al. '09 ($q\bar{q}$ channel)	Feynman diagrams

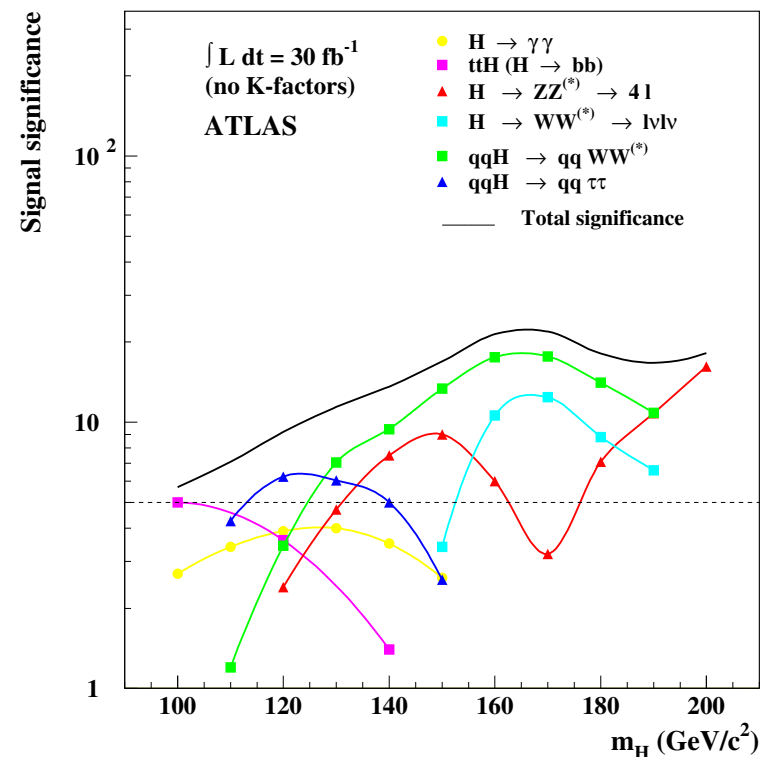
virtual amplitudes for all these $2 \rightarrow 4$ processes: van Hameren, Papadopoulos, Pittau '09

Phenomenological motivation for $pp \rightarrow t\bar{t}b\bar{b} + X$

Spira et al. '98



ATLAS '04



associated production $pp \rightarrow t\bar{t}H$:

- measurement of top Yukawa coupling ($Ht\bar{t}$ coupling)
- early studies: important Higgs-production process for small Higgs-boson masses
- recent studies: **large background renders analysis extremely difficult**
- more experimental and theoretical input needed

Relevance of $t\bar{t}b\bar{b}$ for analysis of $t\bar{t}H$ production

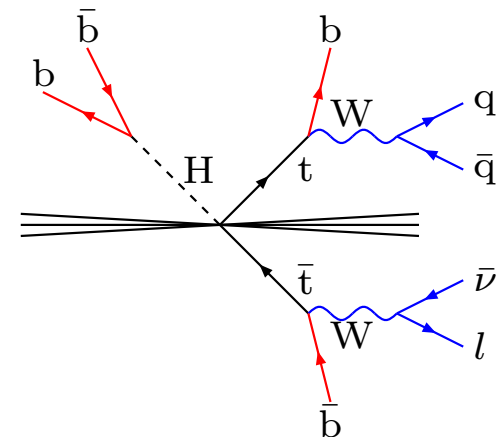
Proposed analysis

- select final state $b\bar{b}b\bar{b}\bar{j}j\nu$ (4 b-quarks!)
- reconstruct $t\bar{t}b\bar{b}$ (b-tagging crucial)
- identify $b\bar{b}$ pair from Higgs decay
- select region $90 \text{ GeV} < m_{b\bar{b}} < 150 \text{ GeV}$

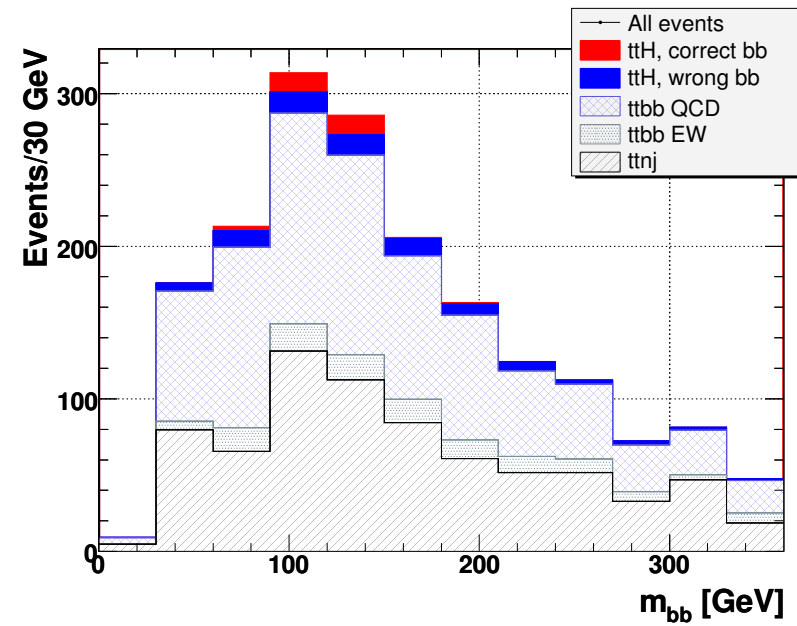
backgrounds

- small S/B (≈ 0.1)
 - O(10%) uncertainty on B kills measurement!
 - dominant B: $t\bar{t}b\bar{b}$ (QCD+EW), $t\bar{t}jj$
 - data do not provide enough precision on normalization and **shape of B**
 - scale dependence at LO $\sim 100\%$
- ⇒ **NLO crucial for reliable B prediction and $t\bar{t}H$ measurement**

Benedetti et al. '07

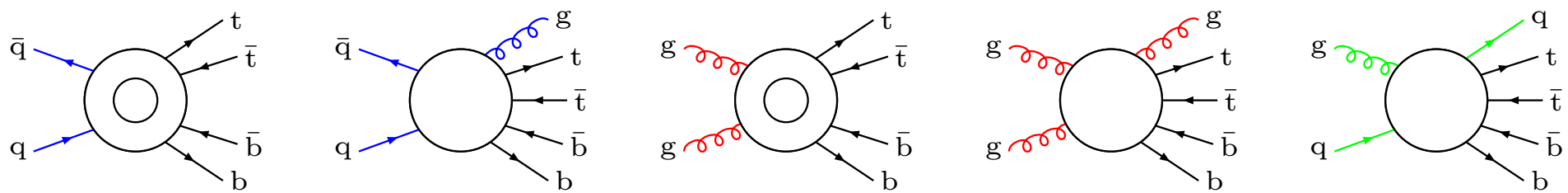


private communication S. Kotov, ATLAS '08

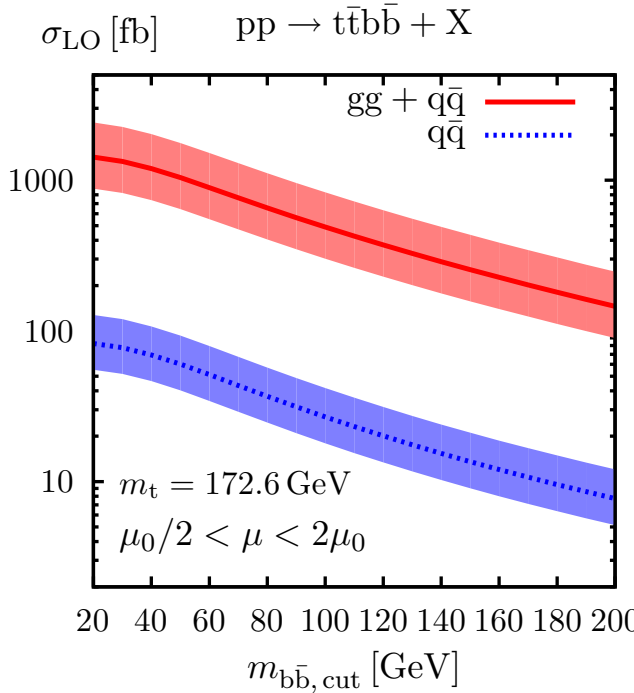


Contributions to $t\bar{t}b\bar{b}$ at NLO

Partonic channels



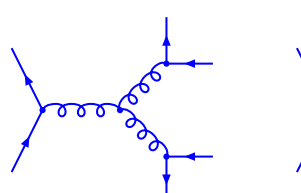
Relative weights and number of Feynman diagrams channels



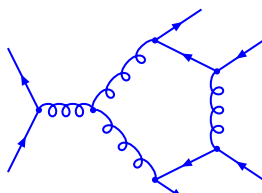
	$q\bar{q}$	gg	qg
# of LO diags	7	36	
# of virtual diags	188	1003	
# of real diags	64	341	64
$(\sigma/\sigma_{\text{tot}})_{\text{LO}}$	5%	95%	
$(\sigma/\sigma_{\text{tot}})_{\text{NLO}}$	3%	92%	5%

Tree and one-loop contributions to $p\bar{p} \rightarrow t\bar{t}b\bar{b} + X$

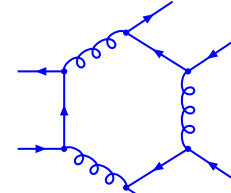
Tree and one-loop diagrams in $q\bar{q}$ and gg channels



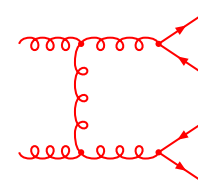
7 trees



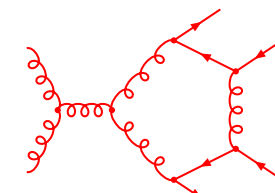
24 pentagons



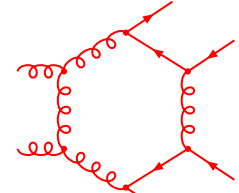
8 hexagons



36 trees



114 pentagons



40 hexagons

two independent calculations

- generation of diagrams with **FeynArts 1.0** and **3.2** Küblbeck et al. '90,'92; Hahn '01
- algebraic simplifications using two independent in-house programs implemented in *Mathematica*, one using **FormCalc 5.2** Hahn '06 for preliminary algebraic manipulations (Dirac algebra, covariant decomposition)

- reduction of tensor integrals according to

Denner, Dittmaier, NPB658 (2003)175 [hep-ph/0212259], NPB734 (2006) 62 [hep-ph/0509141]

→ numerically stable results (two libraries for tensor integrals)

top quarks massive and bottom quarks massless

Algebraic reduction of tensor integrals

Methods developped for $e^+e^- \rightarrow 4f$ Denner, Dittmaier hep-ph/0509141

Avoid instabilities from small Gram determinants in denominators!

- 1- and 2-point integrals: numerically stable direct calculation
- 3-point and 4-point integrals: reduction method depends on phase-space point
(determined on the fly)
 - ▶ phase-space regions without Gram determinant instabilities:
[Passarino–Veltman reduction](#)
 - ▶ otherwise, instabilities are avoided by various alternative reductions
 - [expansions in small determinants](#) (see also R.K.Ellis et al. '05)
 - analytical special cases
 - [semi-numerical method](#) (see also Binoth et al. '05; Ferroglio et al. '02)
(in this calculation for checks only)
- for $N > 4$ use 4-dimensionality of space-time
 - [5-point integrals](#) → five 4-point integrals Melrose '65; Denner, Dittmaier '02, '05
 - [6-point integrals](#) → six 5-point integrals (see also Binoth et al. '05)
 - without inverse Gram determinants and simultaneous reduction of rank by one

Structure of one-loop contributions to $pp \rightarrow t\bar{t}b\bar{b} + X$

Standard matrix elements and colour structures for individual diagram Γ

$$\mathcal{M}^{(\Gamma)} = \underbrace{\mathcal{C}^{(\Gamma)}}_{\text{factorized colour structure}} \sum_m \mathcal{F}_m^{(\Gamma)}(\{p_a \cdot p_b\}) \underbrace{\hat{\mathcal{M}}_m(\{p_a\}, \{\lambda\})}_{\text{standard matrix elements}}$$

form factors $\mathcal{F}_m^{(\Gamma)}$

$$\mathcal{F}_m^{(\Gamma)}(\{p_a \cdot p_b\}) = \sum_{j_1 \dots j_R} \mathcal{K}_{m,j_1 \dots j_R}^{(\Gamma)}(\{p_a \cdot p_b\}) \underbrace{T_{j_1 \dots j_R}(\{p_a \cdot p_b\})}_{\text{tensor loop coefficients}}$$

computed numerically **diagram by diagram** (no analytic reduction to scalar integrals)

many common substructures (tensor integrals, helicity amplitudes) are recycled in the numerical calculation

colour structures

- 6 for $q\bar{q}$ and 14 for gg channels
- **single colour structure for most diagrams** (3 for diagrams with 4g vertex)

cost of colour sums practically reduced to zero

Reduction of standard matrix elements for $\bar{q}q \rightarrow t\bar{t}b\bar{b}$

structure of standard matrix elements (SMEs)

$$\underbrace{\bar{v}(p_1) \dots \gamma^\mu \gamma^\nu \not{p}_3 \dots u(p_2)}_{\text{q}\bar{\text{q}} \text{ chain}} \quad \underbrace{\bar{v}(p_3) \dots \gamma^\mu \gamma^\nu \gamma^\rho \not{p}_6 \dots u(p_4)}_{\text{t}\bar{\text{t}} \text{ chain}} \quad \underbrace{\bar{v}(p_5) \dots \gamma^\rho \not{p}_2 \not{p}_3 \dots u(p_6)}_{\text{b}\bar{\text{b}} \text{ chain}}$$

process-independent identities in D dimensions

- Dirac equation, Dirac algebra, momentum conservation, standard ordering
 $\Rightarrow \mathcal{O}(10^3)$ Dirac structures, still many $\gamma^\mu \otimes \gamma_\mu$ contractions between chains

after cancellation of $1/(D - 4)$ poles use identities in 4 dimensions

- introduce chiral projectors $\omega_\pm = \frac{1}{2}(1 \pm \gamma_5)$ via $u(p_j) \Rightarrow [\omega_+ + \omega_-]u(p_j)$
and exploit identities of type $\gamma^\mu \gamma^\alpha \gamma^\beta \omega_\pm \otimes \gamma_\mu \omega_\mp = \gamma^\mu \omega_\pm \otimes \gamma^\alpha \gamma^\beta \gamma_\mu \omega_\mp$
to exchange Dirac matrices between different Dirac chains

construct a sophisticated, process-dependent algorithm

\Rightarrow reduction of all Dirac structures to ~ 200 SMEs

without introducing new denominators that might spoil numerical stability

Reduction of standard matrix elements for $gg \rightarrow t\bar{t}b\bar{b}$

structure of standard matrix elements (SMEs)

$$\underbrace{\{\epsilon_1^\mu \epsilon_2^\nu, (\epsilon_1 \epsilon_2) p_2^\mu p_4^\nu, (\epsilon_1 p_4)(\epsilon_2 p_3) g^{\mu\nu}, \dots\}}_{\text{gluon polarization vectors}} \underbrace{\bar{v}(p_3) \dots \gamma^\mu \gamma^\rho \cancel{p}_6 \dots u(p_4)}_{t\bar{t} \text{ chain}} \underbrace{\bar{v}(p_5) \dots \gamma^\nu \gamma^\rho \cancel{p}_2 \dots u(p_6)}_{b\bar{b} \text{ chain}}$$

process-independent identities in D dimensions

- $\epsilon_i p_i = 0$, Dirac eq., Dirac algebra, momentum conservation, standard ordering

two alternative reductions in $D = 4$

- **sophisticated method** similarly as for $q\bar{q}$ channel \Rightarrow **502 SMEs**
- less sophisticated and **process-independent reduction** based only on

$$\gamma^{\mu_1} \gamma^{\mu_2} \gamma^{\mu_3} \gamma^{\mu_4} \gamma^{\mu_5} = g^{\mu_1 \mu_2} \gamma^{\mu_3} \gamma^{\mu_4} \gamma^{\mu_5} + \dots + g^{\mu_1 \mu_2} g^{\mu_3 \mu_4} \gamma^{\mu_5} + \dots$$

\Rightarrow **970 SMEs**

result: speed of codes based on both reductions almost identical

\Rightarrow sophisticated process-dependent manipulations not needed for this process

Rational terms from dimensional regularization

Rational terms originate from $1/(D - 4)$ poles of tensor loop integrals

rational terms of UV origin easily obtained via

$$\mathcal{K}_{m,j_1 \dots j_R}^{(\Gamma)}(D) \underbrace{T_{j_1 \dots j_R}}_{\frac{R_{j_1 \dots j_R}}{(D-4)}} = \mathcal{K}_{m,j_1 \dots j_R}^{(\Gamma)}(4) T_{j_1 \dots j_R} + \mathcal{K}'_{m,j_1 \dots j_R}^{(\Gamma)}(4) \mathbf{R}_{j_1 \dots j_R} + \mathcal{O}(D - 4)$$

$$+ T_{j_1 \dots j_R}^{\text{finite}}$$

- UV residues $\mathbf{R}_{j_1 \dots j_R}$ of tensor integrals explicitly available
- easily included in algebraic reduction

rational terms of IR origin arise from double and single IR poles of loop integrals

$$\mathcal{K}_{j_1 \dots j_R}(D) \underbrace{T_{j_1 \dots j_R}}_{\frac{R_{2;j_1 \dots j_R}}{(D-4)^2} + \frac{R_{1;j_1 \dots j_R}}{(D-4)}} \Rightarrow \mathcal{K}'_{j_1 \dots j_R}(4) \mathbf{R}_{1,j_1 \dots j_R} + \frac{1}{2} \mathcal{K}''_{j_1 \dots j_R}(4) \mathbf{R}_{2,j_1 \dots j_R} + \dots$$

$$+ \text{IR-finite part}$$

- can require lot of algebraic work (second-order expansion, many contributions)
- cancel completely in truncated (!) one-loop amplitudes \Rightarrow omit from the start

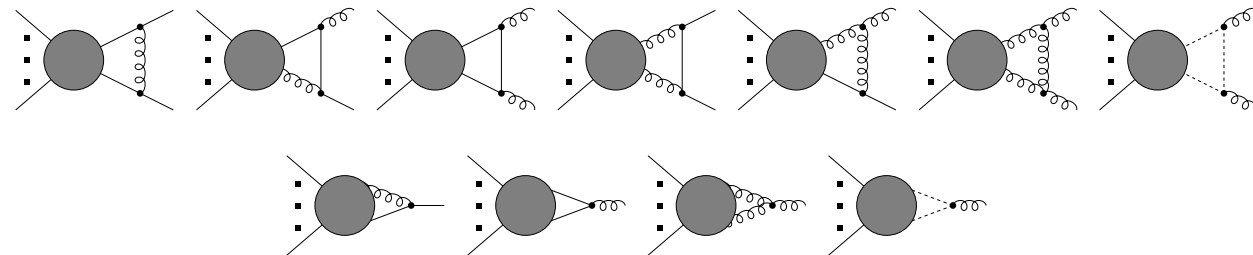
Bredenstein, Denner, Dittmaier, Pozzorini '08 [arXiv:0807.1248]

Cancellation of rational terms of IR origin (sketch of proof)

Rational terms originate from D -dependent $g^{\mu\nu}$ contractions of type $g_{\nu\lambda}\Gamma^{\nu\lambda}$

$$g_{\nu\lambda}g^{\nu\lambda} = D, \quad g_{\nu\lambda}\gamma^\nu \not{p} \gamma^\lambda = (2 - D)\not{p}, \quad \dots$$

- tensor reduction is free of IR rational terms, since soft and collinear singular tensor coefficients do not multiply $g^{\mu\nu}$ ($q^\mu \rightarrow xp^\mu$)
- in all possible diagrams involving IR-divergent integrals

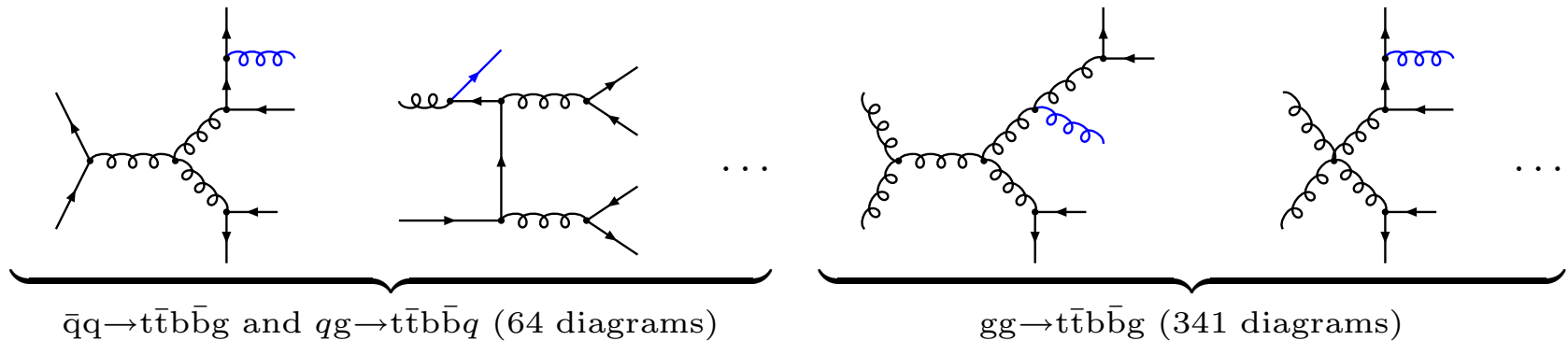


$g_{\nu\lambda}\Gamma^{\nu\lambda}$ contractions cancel in IR regions:

$$\text{Diagram} = \int d^D q \frac{1}{q^2(q+p)^2} \underbrace{\varepsilon^{\mu*}(p) (2q+p)_\mu}_{\rightarrow 0 \text{ in soft/coll. regions}} g_{\nu\lambda}\Gamma^{\nu\lambda}(q) + \dots$$

Real corrections for $pp \rightarrow t\bar{t}b\bar{b} + X$

Diagrams and matrix elements



- with Madgraph 4.1.33 Alwall et al. '07 for all channels
analytically with Weyl–van der Waerden spinors Dittmaier '98 for $q\bar{q}/qg$ channels
numerically with off-shell recursion relations Berends, Giele '88, ... for gg channel

soft and collinear singularities

- regularized dimensionally or with infinitesimal gluon and quark masses
- dipole subtraction Catani, Seymour '96; Catani, Dittmaier, Seymour, Trócsányi '02
30 subtraction terms for $q\bar{q}/gg$ channels and 10 for qg channel
- initial-state collinear singularities cancelled by $\overline{\text{MS}}$ redefinition of PDFs

phase-space integration

- adaptive multi-channel Monte Carlo Berends, Kleiss, Pittau '94; Kleiss, Pittau '94
 $\mathcal{O}(1400)$ channels to map all peaks from propagators (300) and dipoles (1100)

Checks on the calculation for $pp \rightarrow t\bar{t}b\bar{b} + X$

- leading order checked against SHERPA Gleisberg et al. '03
- virtual corrections
 - ▶ cancellation of UV, soft and collinear singularities
 - ▶ independent calculations agree point-wise and after phase-space integration
- real corrections
 - ▶ cancellation of soft and collinear singularities
 - ▶ independent calculations agree point-wise and after phase-space integration
- combination of virtual and real corrections
 - ▶ subtraction terms in independent calculations agree point-wise
 - ▶ independent calculations agree after phase-space integration
 - ▶ results confirmed with two-cutoff slicing in $q\bar{q}$ channel and MADDIPOLE Frederix, Gehrmann, Greiner '08 for gg/qg channel
- two completely independent calculations of all ingredients!

Confirmation by Bevilacqua et al.

Results have been confirmed at per-mille level

Bevilacqua et al., arXiv:0907.4723:

Process	$\sigma_{\text{BDDP}}^{\text{LO}} \text{ [fb]}$	$\sigma_{\text{BCPPW}}^{\text{LO}} \text{ [fb]}$	$\sigma_{\text{BDDP}}^{\text{NLO}} \text{ [fb]}$	$\sigma_{\text{BCPPW}}^{\text{NLO}} \atop \alpha_{max}=1 \text{ [fb]}$	$\sigma_{\text{BCPPW}}^{\text{NLO}} \atop \alpha_{max}=0.01 \text{ [fb]}$
$q\bar{q} \rightarrow t\bar{t}b\bar{b}$	85.522(26)	85.489(46)	87.698(56)	87.545(91)	87.581(134)
$pp \rightarrow t\bar{t}b\bar{b}$	1488.8(1.2)	1489.2(0.9)	2638(6)	2642(3)	2636(3)

Table 1: *Cross sections for $pp \rightarrow t\bar{t}b\bar{b} + X$ at the LHC at LO and NLO for the scale choice $\mu_F = \mu_R = m_t$, from Bredenstein et al. and Bevilacqua et al.. The statistical errors are quoted in parentheses.*

Parton masses

- top mass: $m_t = 172.6 \text{ GeV}$
- bottom mass: $m_b = 0 \text{ GeV}$ (massless approximation better than 3% at LO)

jet definition: k_T algorithm as used at Tevatron run II Blazey et al. '00

- select massless partons (g, q and b) with $|\eta| < 5$
- reconstruct jets with $\sqrt{\Delta\phi^2 + \Delta y^2} > D = 0.4$

cuts for b jets: (motivated by $t\bar{t}H$ analysis)

- require two b-jets with $p_{T,j} > 20 \text{ GeV}$ and $y_j < 2.5$ (b tagging!)
- $b\bar{b}$ invariant mass: $m_{b\bar{b}} > m_{b\bar{b},\text{cut}} = 100 \text{ GeV}$
- top quarks fully inclusive (no decays and no cuts)

NLO settings: [LO obtained with LO α_S , LO PDFs and 1-loop running]

- central scale: $\mu_0 = m_t + m_{b\bar{b},\text{cut}}/2 \Rightarrow \mu_0^2 = m_t \sqrt{p_{T,b} p_{T,\bar{b}}}$
- factor-2 scale variations to estimate LO and NLO scale uncertainty
- PDFs: CTEQ6M with $\alpha_S(M_Z) = 0.118$

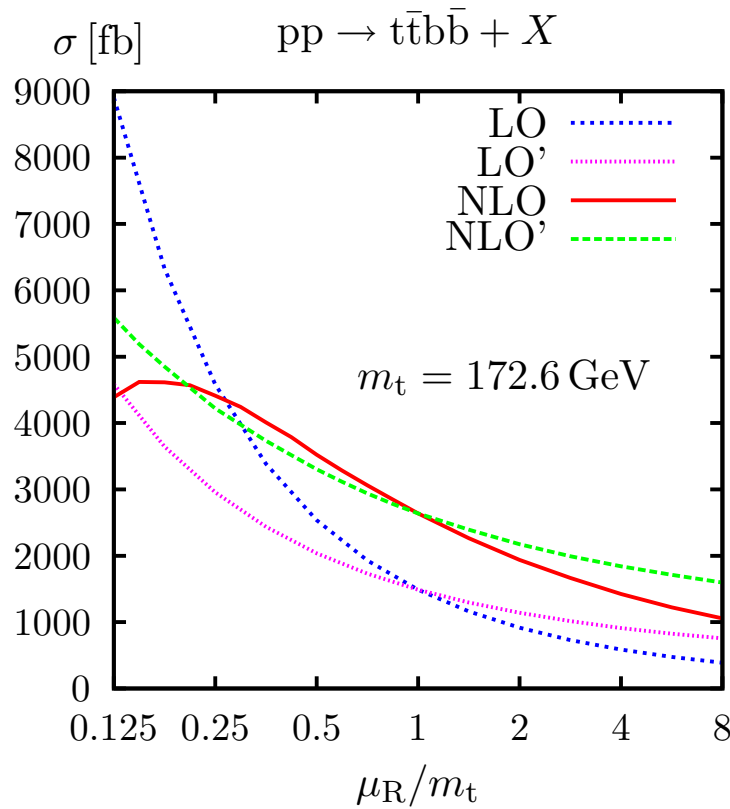
LO and NLO scale dependence for $pp \rightarrow t\bar{t}b\bar{b} + X$

Bredenstein, Denner, Dittmaier, Pozzorini

arXiv:0905.0110

LO, NLO: $\mu_F = \mu_R$

LO', NLO': $\mu_F = m_t^2/\mu_R$



High sensitivity to scale choice

- LO proportional to $\alpha_S(\mu_R)^4$
 $\Rightarrow 70\text{--}80\%$ scale uncertainty

original scale choice based on $t\bar{t}H$ ($K \simeq 1.2$)

$$\mu_0 = E_{\text{thr}}/2 = m_t + m_{b\bar{b}}/2$$

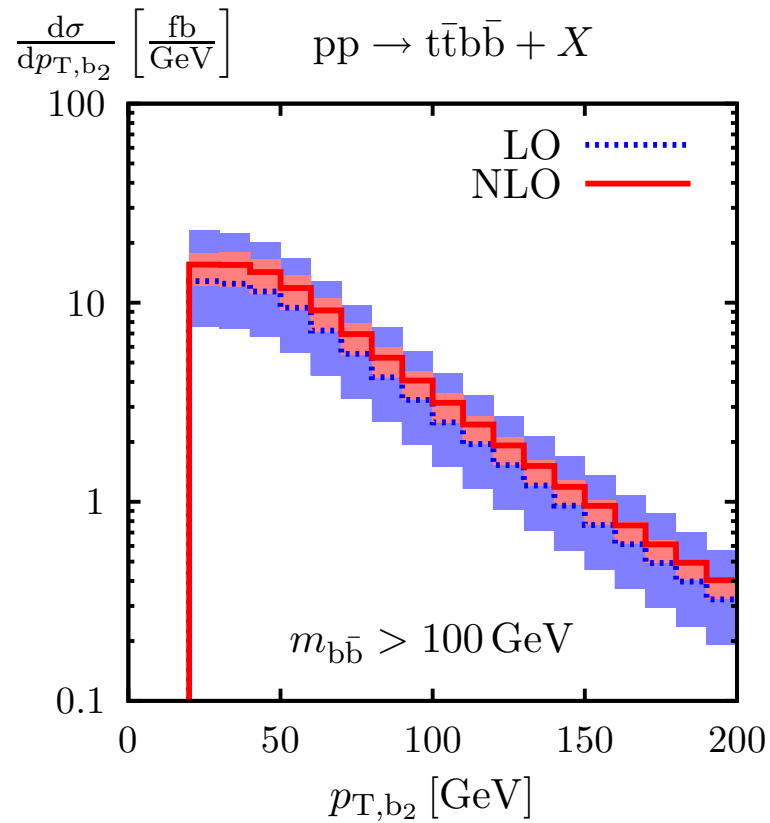
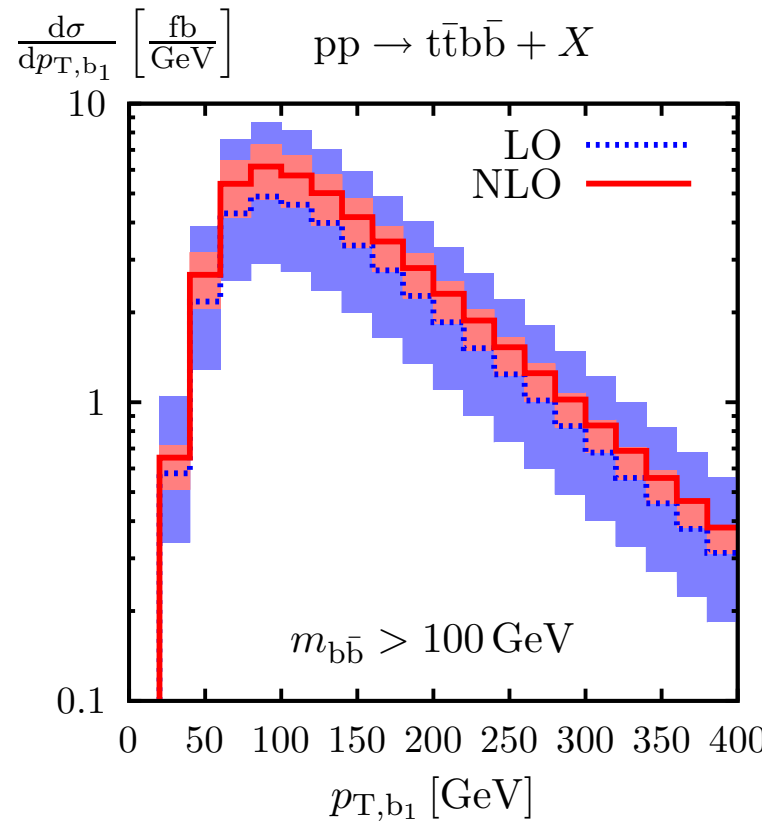
- used by ATLAS assuming $t\bar{t}b\bar{b} \simeq t\bar{t}H$
- yields large K factor (1.8) and scale dependence (34%) ($D = 0.8, m_{b\bar{b},\text{cut}} = 0$)

QCD dynamics of $t\bar{t}H$ and $t\bar{t}b\bar{b}$ different

- $(gg \rightarrow t\bar{t}H) \times (H \rightarrow b\bar{b}) = \mathcal{O}(\alpha_s^2)$
- $(gg \rightarrow t\bar{t}g) \times (g \rightarrow b\bar{b}) = \mathcal{O}(\alpha_s^4)$
- several different channels for $t\bar{t}b\bar{b}$
 \Rightarrow no simple mechanism that fixes scale

Transverse momentum distributions for $\text{pp} \rightarrow t\bar{t}b\bar{b} + X$

Bredenstein, Denner, Dittmaier, Pozzorini



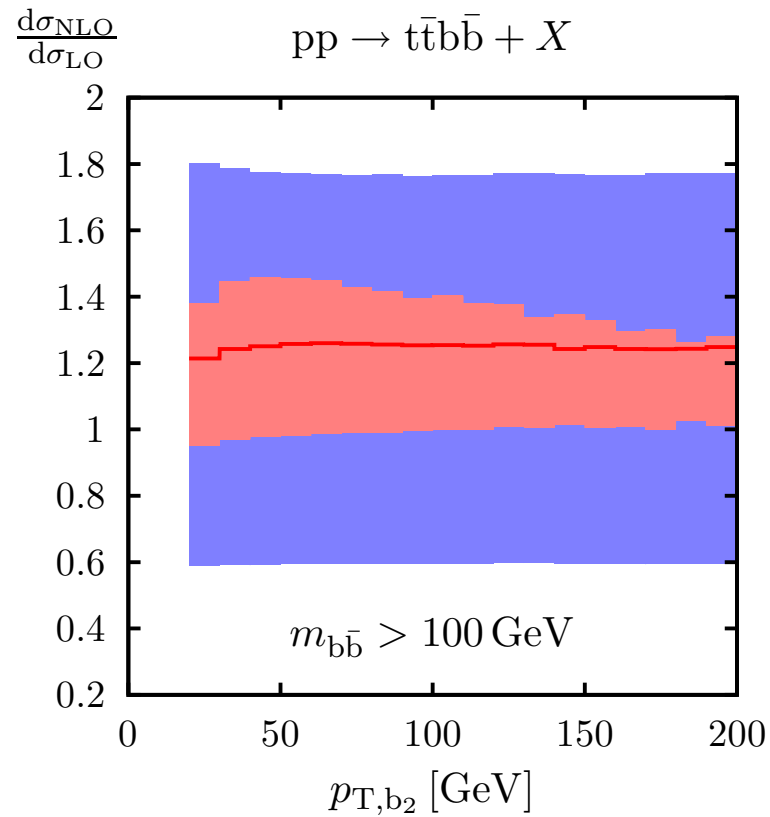
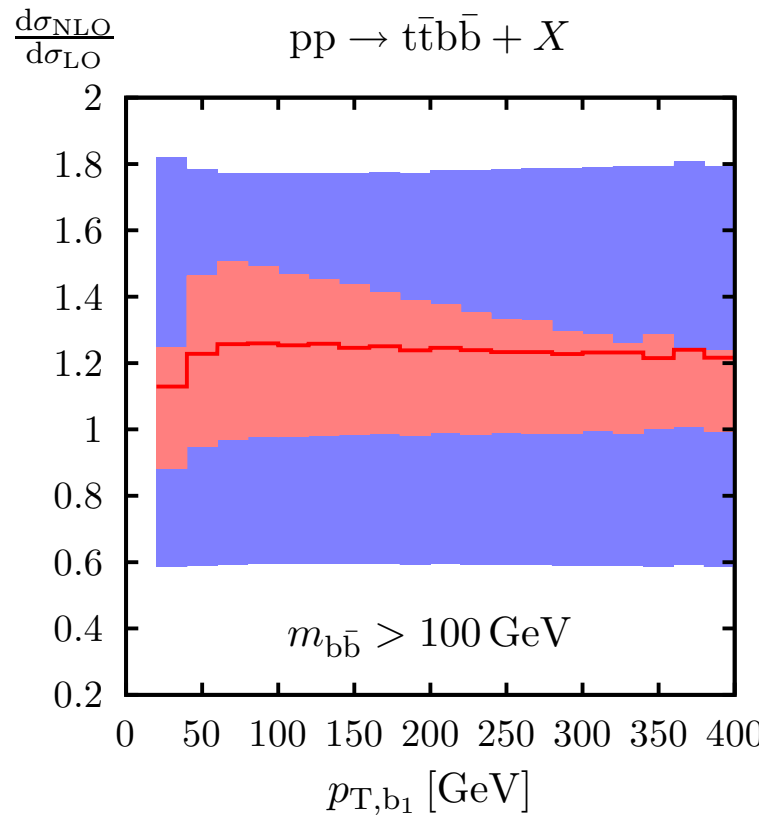
b-jets have typically $p_{T,b} \ll m_t$ and rather different distributions

- harder b jet (left) peaks at $p_{T,b} \sim 100 \text{ GeV}$
- softer b jet (right) tends to saturate cut at 20 GeV

introduce effective scale $\mu_0^2 = m_t \sqrt{p_{T,b} p_{T,\bar{b}}}$

Transverse momentum distributions for $pp \rightarrow t\bar{t}b\bar{b} + X$

Bredenstein, Denner, Dittmaier, Pozzorini

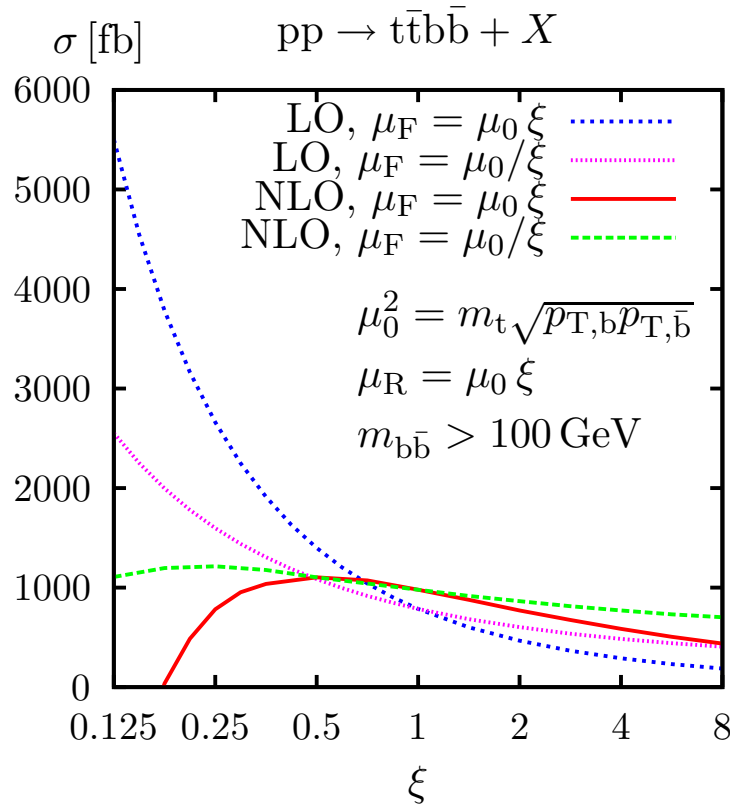


New scale choice improves convergence:

- NLO band perfectly fits within LO band: $K \simeq 1.25$
- K -factor almost constant over wide $p_{T,b}$ range for both b quarks
- NLO scale uncertainty reduced to about 20%

LO and NLO scale dependence for $pp \rightarrow t\bar{t}b\bar{b} + X$

Bredenstein, Denner, Dittmaier, Pozzorini
arXiv:1001.4006



Variations around new central scale

$$\mu_0^2 = m_t \sqrt{p_{T,b} p_{T,\bar{b}}}$$

good news for theory: improved convergence

- small correction and uncertainty:
 $K = 1.24 \pm 21\%$
- central scale close to a maximum

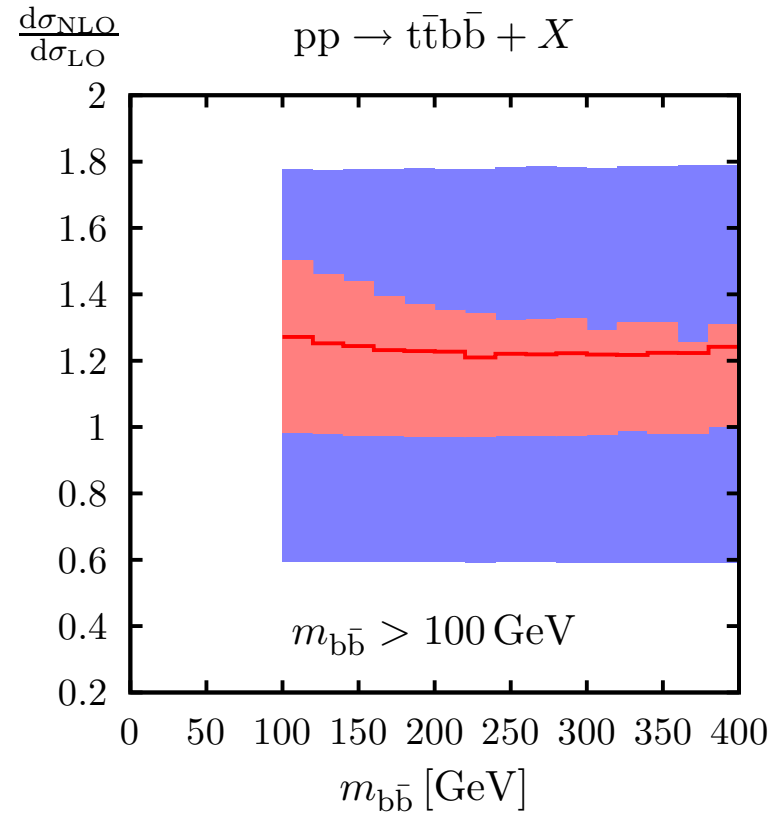
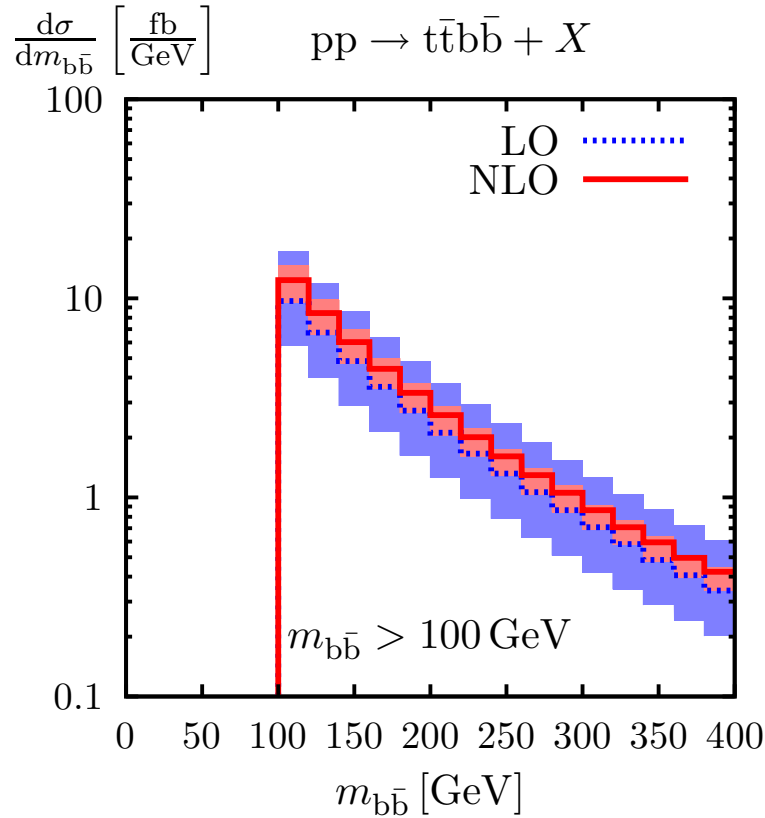
bad news for experiment:
enhancement of $t\bar{t}b\bar{b}$ background

- already large for old scale $\mu_{\text{old}} = E_{\text{thr}}/2$:
 $K \simeq 1.8$
- even worse with new scale
($\sigma_{\text{NLO}}(\mu_0)/\sigma_{\text{LO}}(E_{\text{thr}}/2) \simeq 2.18$)
since $\mu_0 \simeq 0.5\mu_{\text{old}}$
(in spite of smaller K factor)

b \bar{b} invariant-mass distribution for pp $\rightarrow t\bar{t}b\bar{b} + X$

crucial observable for t $\bar{t}H$ production

Bredenstein, Denner, Dittmaier, Pozzorini

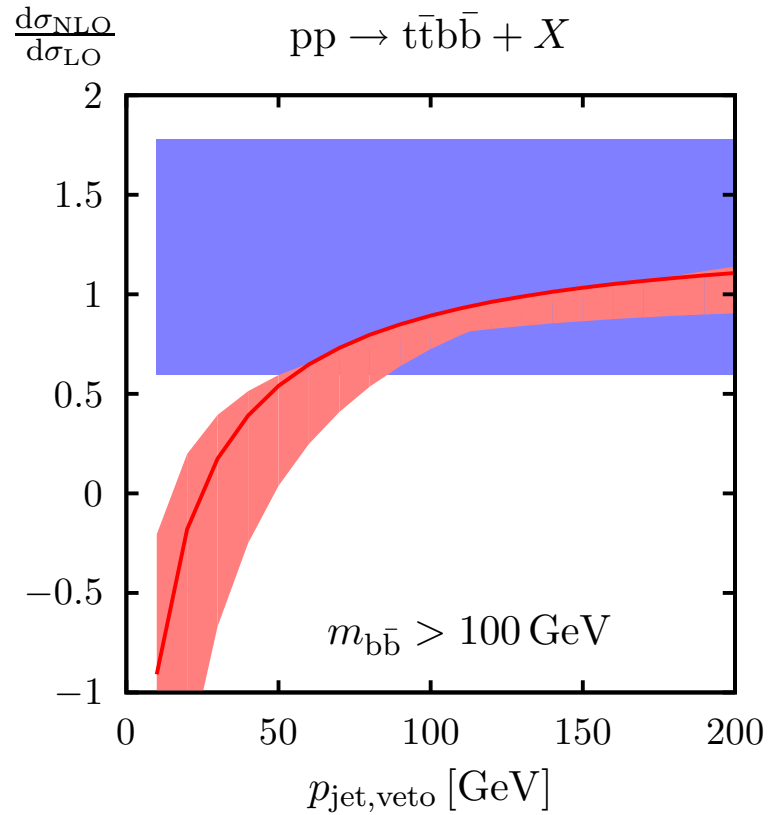
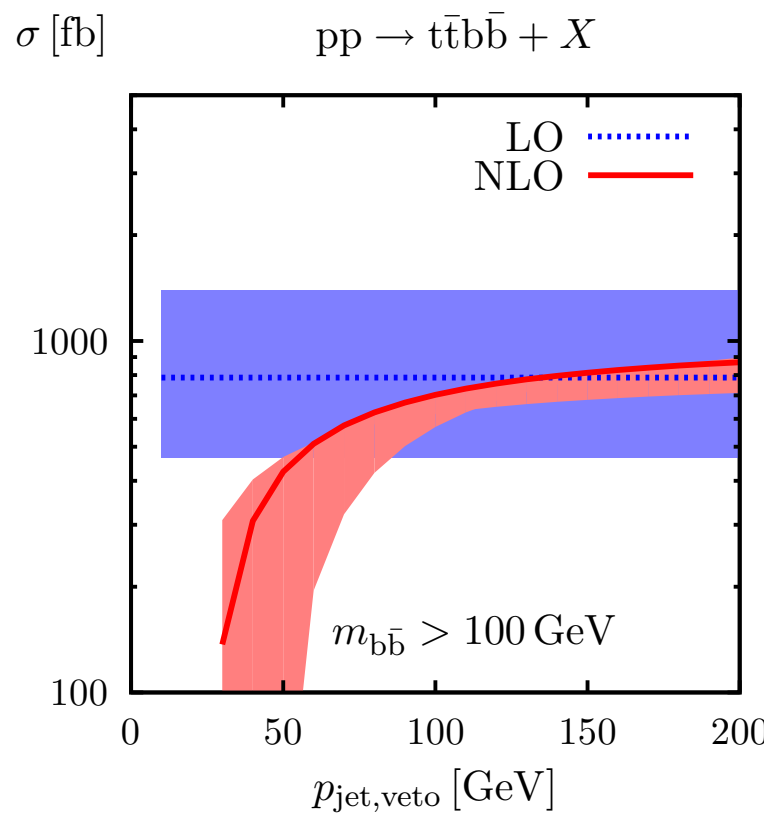


- small NLO correction $K \simeq 1.24$
- K -factor almost constant over wide $m_{b\bar{b}}$ range
- NLO scale uncertainty $\sim 20\%$

Effect of a jet veto for $pp \rightarrow t\bar{t}b\bar{b} + X$

Jet veto could reduce large $t\bar{t}b\bar{b}$ background

Bredenstein, Denner, Dittmaier, Pozzorini



- perturbative instability for small $p_{jet,veto}$ ($\lesssim 50$ GeV)
- safe jet-veto values $p_{jet,veto} \sim 100$ GeV ($\Rightarrow 30\%$ reduction in cross section)
 - ▶ K factor reduced from $K = 1.24$ to $K \simeq 0.9$
 - ▶ NLO scale uncertainty hardly affected ($\sim 19\%$)

Speed and precision of calculation

Runtime and statistical precision with 3 GHz Intel Xeon processor

	$\sigma/\sigma_{\text{LO}}$	# events (after cuts)	$(\Delta\sigma)_{\text{stat}}/\sigma$	runtime	time/event
tree level	86%	5.3×10^6	0.4×10^{-3}	38 min	0.4 ms
virtual	-11%	0.26×10^6	0.6×10^{-3}	13 h	180 ms
real + dipoles	49%	10×10^6	3×10^{-3}	40 h	14 ms
total	124%		4×10^{-3}	53 h	

- 2 CPU days $\Rightarrow \mathcal{O}(10^7)$ events and $\mathcal{O}(10^{-3})$ statistical uncertainty for σ_{tot} (distributions obtained with $\sim 5 \times 10^8$ events after cuts)
- speed of virtual corrections remarkably high: 180 ms/event (including colour and polarizations sums)
- for same precision ($\Delta\sigma/\sigma$) virtual corrections require less CPU-time than real corrections (scale-dependent statement!)

Conclusions

NLO QCD calculation for $pp \rightarrow t\bar{t}b\bar{b} + X$ at the LHC

- very important for $t\bar{t}H$ measurement at LHC
- $2 \rightarrow 4$ LHC process with highest priority on 2005 Les Houches wishlist
- calculation performed by two different groups with completely different methods
agreement at per-mille level

QCD scale used by ATLAS not adequate \Rightarrow replaced by new scale

- stabilizes QCD prediction: $K = 1.8 \pm 34\% \Rightarrow K = 1.25 \pm 21\%$
- cross section by factor 2 larger as assumed in ATLAS studies

Technical test of diagrammatic tensor-reduction approach

- remarkably high CPU speed
- very good perspectives to study other six-particle processes

Backup slides

Standard matrix elements for $\bar{q}q \rightarrow t\bar{t}b\bar{b}$

25 types of standard matrix elements (polarization dependent)

- 10 of "massless" type: one Dirac matrix per chain

$$\bar{v}(p_1) \cancel{p}_i \omega_\alpha u(p_2) \quad \bar{v}(p_3) \gamma^\mu \omega_\beta u(p_4) \quad \bar{v}(p_5) \gamma^\mu \omega_\rho u(p_6)$$

$$\bar{v}(p_1) \cancel{p}_i \omega_\alpha u(p_2) \quad \bar{v}(p_3) \cancel{p}_j \omega_\beta u(p_4) \quad \bar{v}(p_5) \cancel{p}_k \omega_\rho u(p_6)$$

- 15 of "massive" type: 2/0 Dirac matrices inside the $t\bar{t}$ chain*

$$\bar{v}(p_1) \cancel{p}_i \omega_\alpha u(p_2) \quad \bar{v}(p_3) \cancel{p}_j \gamma^\mu \omega_\beta u(p_4) \quad \bar{v}(p_5) \cancel{p}_k \omega_\rho u(p_6)$$

$$\bar{v}(p_1) \gamma^\mu \omega_\alpha u(p_2) \quad \bar{v}(p_3) \cancel{p}_j \cancel{p}_j \omega_\beta u(p_4) \quad \bar{v}(p_5) \gamma^\mu \omega_\rho u(p_6)$$

$$\bar{v}(p_1) \gamma^\mu \omega_\alpha u(p_2) \quad \bar{v}(p_3) \gamma^\mu \gamma^\nu \omega_\beta u(p_4) \quad \bar{v}(p_5) \gamma^\nu \omega_\rho u(p_6)$$

$$\bar{v}(p_1) \gamma^\mu \omega_\alpha u(p_2) \quad \bar{v}(p_3) \omega_\beta u(p_4) \quad \bar{v}(p_5) \gamma^\mu \omega_\rho u(p_6)$$

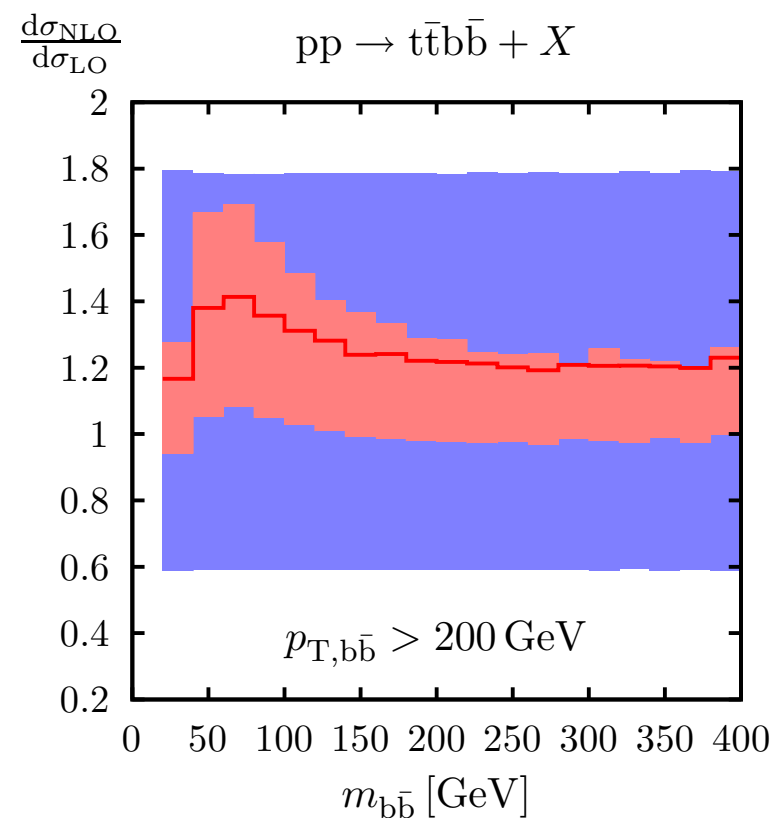
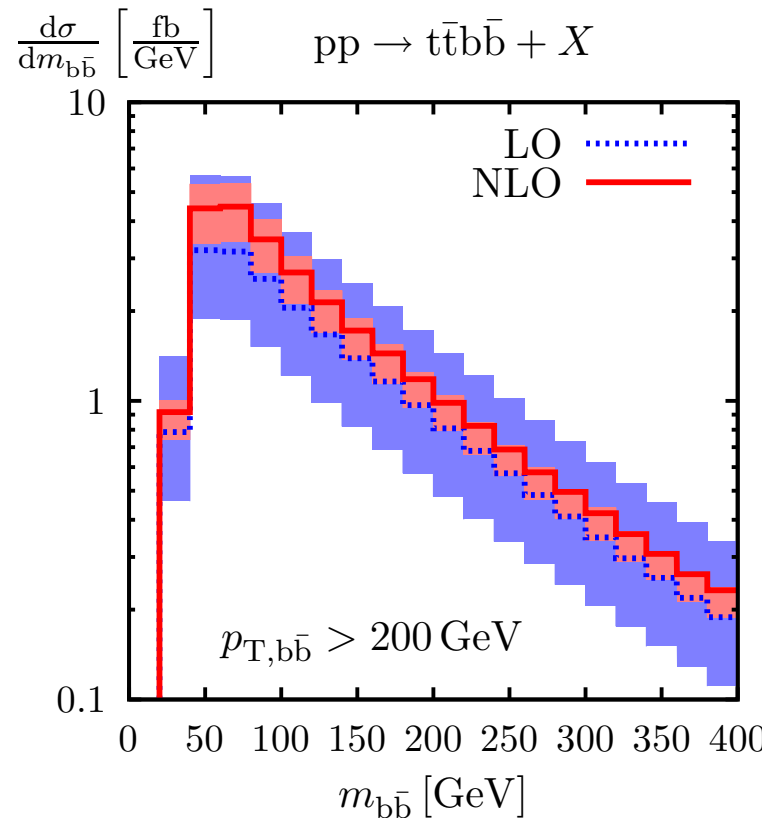
$$\bar{v}(p_1) \cancel{p}_i \omega_\alpha u(p_2) \quad \bar{v}(p_3) \omega_\beta u(p_4) \quad \bar{v}(p_5) \cancel{p}_k \omega_\rho u(p_6)$$

*price to pay for the presence of massive top quarks

b \bar{b} invariant-mass distribution for pp $\rightarrow t\bar{t}b\bar{b} + X$

Setup with highly boosted b \bar{b} pairs: $p_{T,b\bar{b}} > 200 \text{ GeV}$ (instead of $m_{b\bar{b}} > 100 \text{ GeV}$)

Bredenstein, Denner, Dittmaier, Pozzorini



- small NLO correction $K \simeq 1.31$
- NLO corrections distort shape by about 20%
- NLO scale uncertainty $\sim 20\%$